RSC Advances

This is an *Accepted Manuscript*, which has been through the Royal Society of Chemistry peer review process and has been accepted for publication.

Accepted Manuscripts are published online shortly after acceptance, before technical editing, formatting and proof reading. Using this free service, authors can make their results available to the community, in citable form, before we publish the edited article. This *Accepted Manuscript* will be replaced by the edited, formatted and paginated article as soon as this is available.

You can find more information about *Accepted Manuscripts* in the Information for Authors.

Please note that technical editing may introduce minor changes to the text and/or graphics, which may alter content. The journal's standard Terms & Conditions and the Ethical guidelines still apply. In no event shall the Royal Society of Chemistry be held responsible for any errors or omissions in this *Accepted Manuscript* or any consequences arising from the use of any information it contains.

ROYAL SOCIETY OF CHEMISTRY

www.rsc.org/advances

Interactions of the aquated forms of ruthenium (III) anticancer drugs with protein: A detailed Molecular docking and QM/MM investigation

Dharitri Das, Abhijit Dutta and Paritosh Mondal*

Department of Chemistry, Assam University, Silchar 788011, Assam, India

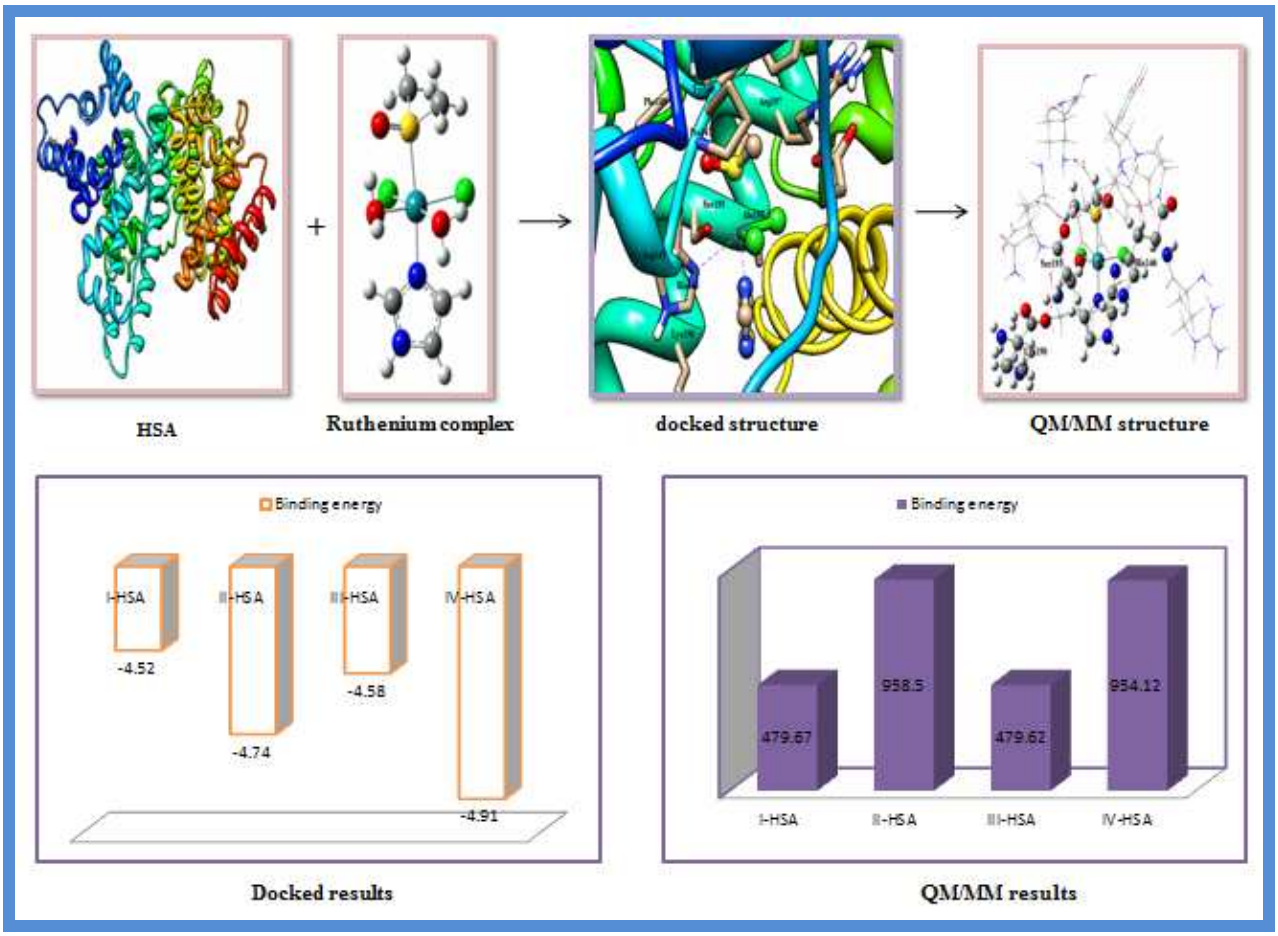

RSC Advances Accepted Manuscript

Interactions of the aquated forms of ruthenium (III) anticancer drugs with protein: A detailed Molecular docking and QM/MM investigation

Dharitri Das, Abhijit Dutta, Paritosh Mondal*

Department of Chemistry, Assam University, Silchar 788011, Assam, India

*Corresponding author. Email: paritos_au@yahoo.co.in

Abstract

Interaction of monooaqua and diaqua ruthenium complexes such as, [trans-$RuCl_3(H_2O)$(3H-imidazole)(dmso-S)] **I**, [trans-$RuCl_2(H_2O)_2$(3H-imidazole)(dmso-S)]$^{+1}$ **II**, [trans-$RuCl_3(H_2O)$(4-amino-1,2,4-triazole)(dmso-S)] **III** and trans-$RuCl_2(H_2O)_2$(4-amino-1,2,4-triazole)(dmso-S)]$^{+1}$ **IV**, which are formed after intracellular aquation of their respective complexes, with human serum albumin (**HSA**) has been computationally investigated by molecular docking and two layer QM/MM hybrid methods. The computed binding energy of monoaqua adduct **I-HSA** and **III-HSA** evaluated by docking simulation are found to be -4.52 kcalmol^{-1} and -4.58 kcalmol^{-1} whereas the binding energy of diaqua adducts **II-HSA** and **IV-HSA** are evaluated to be -4.74 kcalmol^{-1} and -4.91 kcalmol^{-1}, respectively. Docking results also show that the ruthenium atoms of all the complexes are actively involved in coordination with histidyl nitrogen atoms in the active site of protein. In addition, in order to probe the stabilities of monoaqua and diaqua ruthenium complexes in the active site of protein, we have calculated their energetic by two layer QM/MM method. QM/MM study suggests higher stability of diaqua adduct, **II-HSA**. The stability of adducts varies in the order: **II-HSA> IV-HSA**> **I-HSA**> **III-HSA**. Binding energy values of all the complexes increase with the incorporation of solvent effect. Thus molecular docking and QM/MM results show that ruthenium complexes interact with the protein receptor more rapidly after their second hydrolysis. Hence, docking as well as ONIOM results will be highly beneficial for providing insight into the molecular mechanism of ruthenium complexes with protein receptor.

Keywords: DFT, ruthenium (III) complexes, Docking, ONIOM

RSC Advances Accepted Manuscript

Introduction

Platinum complexes like cisplatin, carboplatin, oxaliplatin etc. are the most commonly used anticancer agents in chemotherapeutic treatment for last thirty years. However, high toxicity and undesirable side effects of these complexes[1-2] lead to the discovery of new metal based anticancer agents[3-4]. Among the other metal complexes, ruthenium complexes are found to be effective alternatives to platinum.[5-6] Two Ru(III) complexes, NAMI-A and KP1019 are currently in phase II clinical trials.[7-8] NAMI-A has shown its activity against cancer metastases[9] while KP1019[10] is effective towards primary cancers. Antimetastatic agents are extremely important in the treatment of cancer because 90 percent of cancer deaths are reported to be due to metastasis formation. NAMI-A complex is very unstable at physiological conditions like pH 7.4, [Cl] =0.1 M, 37 °C. It has undergone hydrolysis after dissolution[11-14] and subsequent dissociation of chloride or DMSO ligand leading to the formation of diaqua derivatives.[12] It has been investigated further that dissociation process gives rise to formation of ruthenium complexes with only one imidazole and one chlorido ligands.[14] Hence to enhance hydrolytic stability, infusion solution of NAMI-A is dissolved in physiological concentration of sodium chloride, when given to patients.[15]

Over the past 25 years, a large number of studies have been carried out in order to clarify the mechanism of action of ruthenium complexes towards biomolecular target. In general, increasing evidences in the literature show that mechanism responsible for anticancer activities of ruthenium complexes are based on their DNA nucleobases interaction.[16-18] But before such interaction occurs, these complexes should be passed from cellular memebrane to the nuclear memebrane. During this time ruthenium complexes may interact with many active sites such as proteins, peptides and other molecular targets.[19-21] It is well-recognized that ruthenium complexes interact with protein receptor immediately after its intravenous administration.[22-23] Transferrin, which is mainly responsible for transporting iron to the body cells could be employed as a natural carrier for delivering cytotoxic ruthenium agents to tumor cells because of their higher demand for iron.[24-25] On the other hand albumin, a most abundant human plasma protein displays high binding affinity[26] and act as a reservoir for the transferrin cycle. Lots of efforts have been devoted for investigating the interactions between ruthenium complexes and proteins. It is believed that ruthenium complexes tend to coordinate N-side chains of amino acids like histidine, arginine as well as other amino acids, since these complexes are known to bind selectively to imine sites in biomolecules.[27-28] Also there are evidences for binding of ruthenium to sulfur (S donor/thiolate) compounds, but these complexes are kinetically unstable, especially in the presence of oxygen.[29-30] The interactions are generally facilitated by aqua derivatives of ruthenium (III) complexes because these derivatives are much more reactive towards intracellular target as compared to their parent chloro

RSC Advances Accepted Manuscript

complexes. In case of NAMI-A, very interesting information have been obtained when crystal structures of lactoferrin—NAMI-A[31] and carbonic anhydrase —NAMI-A adducts[32] are examined. The crystal structure of carbonic anhydrase—NAMI-A adduct reveals that ligands of ruthenium complex are progressively lost during protein binding and in final adduct ruthenium complex retains its octahedral arrangement completed by water molecules, imidazolium nitrogen atom of His64 and carbonyl oxygen atom of Asn62 .[32] Recently, Vergara *et al*.[33] has investigated the binding properties of a new NAMI-A analogue called azi-Ru, which is more cytotoxic and shows higher antiproliferative activity than NAMI-A towards hen egg lysozyme (HEWL). They have reported that azi-Ru binds with the protein lysozyme through His15 and Asp87 amino acid residue. So far, numbers of experimental researches on mode of action of ruthenium-based drugs (including the hydrolysis mechanism and binding to biomolecules) have been done but to the best of our knowledge only a few computational studies have been performed at the molecular level.[34] Besker *et.al.*[35] have published a DFT study on binding nature of antitumor ruthenium (II) and ruthenium (III) complexes with DNA and protein. It is found that N7 of guanine, histidyl imidazole residue and sulfur containing methionine and cysteine residues are the preferred binding sites for ruthenium complexes. Chen *et al.*[36] has investigated the two step hydrolysis reaction of NAMI-A by DFT method where they found that chloroaquated and cis diaquated species of NAMI-A is thermodynamically more stable than corresponding trans diaquated species. Recently, many studies have reported the stepwise mechanism of interaction of monoaquated and diaquated species of metal complexes with DNA and protein residues.[37-39]

Present work examines the stability and binding affinity of monoaqua and diaqua complexes of NAMI-A: [trans-$RuCl_3(H_2O)$(3H-imidazole)(dmso-S)](**I**), [trans-$RuCl_2(H_2O)_2$(3H-imidazole)(dmso-S)]$^{+1}$ (**II**) and its amino derivative: [trans-$RuCl_3(H_2O)$(4-amino-1,2,4-triazole)(dmso-S)] (**III**) and trans-$RuCl_2(H_2O)_2$(4-amino-1,2,4-triazole)(dmso-S)]$^{+1}$ (**IV**) with human serum albumin (**HSA**). Currently, it is not clear whether monoaqua or diaqua complexes or both of them are active species before reaction with protein receptor. Therefore we have considered both monoaqua and diaqua form of ruthenium (III) complexes for protein interaction. In order to find out the stability and binding affinity of anticancer drugs with protein receptor, many researchers have utilized two powerful computational strategies: docking and ONIOM (Our own N-layered Integrated molecular Orbital and Molecular Mechanics).[40-42] In the current study , to find out the appropriate orientation of the metal complex into the binding site of protein receptor, molecular docking simulations are taken up in an initial step and then quantum chemical calculations are performed using two layer ONIOM method.

Computational Details

Structure

RSC Advances Accepted Manuscript

DFT optimized geometry of **I**, **II, III** and **IV** complexes in gas phase are obtained using unrestricted Becke's[43] three parameter hybrid exchange functional (B3) and the Lee-Yang-Parr correlation functional (LYP) (B3LYP)[44] functional with LANL2DZ + 6-31G (d,p) basis sets. LANL2DZ basis set[45] which describe effective core potential of Wadt and Hay (Los Alamos ECP) on ruthenium atom and 6-31G(d,p) basis set[46] for all other non metal atoms are used for ground state geometry optimization. LANL2DZ basis set is used as it reduces the calculation time containing larger nuclei. Vibrational analysis has been performed at the same level of theory for achieving energy minimum. GAUSSIAN 09 program package[47] is employed to carry out all the DFT calculations.

Molecular docking simulation

DFT optimized structure of ruthenium complexes such as **I**, **II**, **III** and **IV** and crystal structure of human serum albumin (**HSA**) entitled 1H9Z, obtained from research collaboratory for structural bioinformatics (RCSB) protein data bank are taken for molecular docking simulation. The three homologous domains of **HSA** are 1, 2, 3 each of which is composed of A and B subdomains.[48] Site 1 and site 2, located in hydrophobic cavities in subdomains 2A and 3A are the two major drug binding site of HSA.[48-49] Some recent investigations have demonstrated that anthanthracycline drugs bind to a non classical binding site on subdomain 1B of **HSA**.[50-51] Therefore in this study, subdomain 1B has been chosen as ligand binding site during docking simulation. Autodock 4.2 program[52], an interactive molecular graphics program is used to perform molecular docking simulation. For docking, the protein structure in pdb format is prepared by structure preparation tool available in Auto Dock Tools package version 1.5.4. All the water molecules and the residues (warfarin moieties namely Coumarin, Benzyl and Acetonyl which are found to be complexed with **HSA** receptor) have been removed from the crystal structure of **HSA** and then polar hydrogen atoms are added for saturation, Gasteiger charges are computed and non-polar hydrogen atoms are merged. A grid box with grid spacing of 0.375 Å and dimension of 60×60×60 grid points along x, y and z axes are built around the ligand binding site. The grid box carries the complete binding site of the protein receptor and gives sufficient space for the ligand translational and rotational walk. Finally, ten possible docking runs are performed with step sizes of 2 Å for translation and 50^0 for rotation. A maximum number of energy evaluations are set to 25000 and a maximum number of 27000 GA operations are generated with an initial population of 150 individuals. The rate of gene mutation and crossover are set to 0.02 and 0.80, respectively.

QM/MM calculation

The lowest energy structure, obtained from preceding docking simulation is chosen as the starting geometry for the two layer ONIOM study. The residues located outside the active site region of protein receptor are removed in order to reduce the system size. Investigation of the whole protein-ligand adduct by quantum mechanics (QM) is very computationally demanding. Hence, we have applied QM on

RSC Advances Accepted Manuscript

the interacting residues with the ruthenium complex and molecular mechanics (MM) for the remaining part of the system (Fig.1). For monoaquated adduct, the QM region is composed of ruthenium complex, His146 and Gln459 residue while MM region is composed of Ala194, Arg145, Arg197, Asp108, Glu425, Leu463, Phe149, Pro147, Ser193 and Tyr148 residue respectively. Here charge of both the layer is set to be 0. On the other hand, for diaquated adducts, QM part includes ruthenium complex, His146 and Ser193. Along with these two residues Lys190 (for **II-HSA**), Pro147 and Glu425 (for **IV-HSA**) are included in the QM layer. The charge of QM set for diaquated adduct is set to be +1. Finally, the whole structure is optimized using two layer ONIOM method by treating QM region at UB3LYP/ (LANL2DZ+6-31G (d,p)) level. MM region is described using universal force field, implemented in GAUSSIAN 09 program. In the two layers ONIOM method, the total energy (E_{ONIOM}) of the entire system is obtained from three independent energy calculations:

$$E^{ONIOM2} = E^{\text{high}}_{\text{model system}} + E^{\text{low}}_{\text{real system}} - E^{\text{low}}_{\text{model system}}$$

Real system contains full geometry of the molecule and is considered as MM layer while the model system contains the chemically most important (core) part of the system that is considered as QM layer.

To find the relative stability of respective adducts, we have evaluated the interaction energy, ΔE, which is given by the expression:

$$\Delta E = \Delta E_{HSA/Ru-complex} - \Delta E_{HSA} - \Delta E_{Ru-complex}$$

$\Delta E_{HSA/Ru-complex}$ is the energy of the optimized adduct of complex-HSA, ΔE_{HSA} is the energy of the optimized HAS receptor and the $\Delta E_{Ru-complex}$ is the energy of the optimized ruthenium complexes.

To observe effect of solvation in the ruthenium complex**—HSA** interaction, single-point calculations have been performed on the interacting part of the protein by the UB3LYP functional, using LANL2DZ and 6-31G(d,p) basis sets and conductor-like polarized continuum model.[53-54] In order to reduce the calculation time, we have taken only the high level (QM) part for single point calculation.

Results and Discussion

Structural analysis of monoaqua and diaqua complexes

Important geometrical parameters of the ruthenium complexes evaluated in gas phase are presented in Table1 and their optimized geometries evaluated by DFT at B3LYP level are shown in Fig. 2. In complex **I**, the Ru—Cl1, Ru—Cl2, Ru—Cl3, Ru—O, Ru—N and Ru—S bond lengths are calculated to be 2.43 Å, 2.38 Å, 2.34 Å, 2.21 Å, 2.10 Å and 2.36 Å respectively. Ru—O bond length is found to be shorter than that of Ru—Cl bond lengths, indicating the stronger coordination ability of water

RSC Advances Accepted Manuscript

ligands than that of chloride ligands. The coordinated water molecule of complex **I** form a hydrogen bond with DMSO oxygen atom (1.85 Å). The bond angles Cl_1—Ru—O(wat1), O(wat1)—Ru—Cl_2 , Cl_2—Ru—Cl_3 and Cl3—Ru—Cl1 of the complex **I** are found to be as: 80.6^0, 86.3^0,97.2^0 and 95.7^0, respectively. As a consequence of this deviation of bond angles from 90^0, the geometry about the ruthenium atom is distorted from regular octahedral structure. For complex **II**, ruthenium atom is coordinated with two water molecules and one of the two water molecules have formed hydrogen bonding interaction with DMSO oxygen atom within a distance of 1.70 Å. Ru—O(wat1) and Ru—O(wat2) bond lengths are found to be 2.23 and 2.16 Å, respectively. Complex **II** also exhibits pseudooctahedral configuration having Cl_1—Ru—O(wat1), O(wat1)—Ru—O(wat2), $(wat2)_2$—Ru—Cl_3 and Cl3—Ru—Cl1 bond angles are in the range of 83.9^0—99.8^0. These geometrical parameters are comparable with available experimental data. Similar geometrical parameters are also reported by Chen *et al.* on studying the aquation of NAMI-A.[36] However, slightly higher values of bond lengths of all complexes are thought to be due to systematic errors caused by computation method, basis set and environment factors.[36] Electronic structures of complex **III** and complex **IV** are found to be similar to that of complex **I** and complex **II.**

Stability of the ruthenium complexes

Chemical properties of ruthenium complexes are determined by analyzing the nature of highest occupied molecular orbital (HOMO) and the lowest unoccupied molecular orbital (LUMO). Calculated LUMO and HOMO energies of the ruthenium complexes are listed in Table 2. With the help of LUMO—HOMO energy separation, the kinetic stability and relative reactivity pattern of a chemical system can be predicted. The lower value of energy separation indicates higher reactivity and lower kinetic stability of a molecule.[55] Pearson pointed out that the LUMO—HOMO energy separation represents the chemical hardness which is a reliable reactivity parameter to predict the stability of a molecule.[56] Greater stability of molecules is due to their higher hardness value as stated by maximum hardness principle.[57] It is observed from computational investigation that complex **II** (Table 2) having higher value of LUMO—HOMO energy gap as well as higher chemical hardness value, exhibits higher stability than that of complex **I**, **III** and **IV**.

Docking study

The analysis of molecular docking calculations between ruthenium complexes with **HSA** shows that all the complexes exhibit almost similar binding orientation. The interaction energy of all the protein adducts along with their experimental binding constant (metal complexes binding to albumin) [58] are reported in Table 3. The binding energy for **I-HSA**, **II-HSA**, **III-HSA** and **IV-HSA** adducts are evaluated to be -4.52, -4.74, -4.58 and -4.91 kcal mol^{-1}. The larger negative value of binding energy reflects greater

RSC Advances Accepted Manuscript

binding affinity of ruthenium complexes with the protein receptor. The most important amino acid components involved in binding interaction with protein receptor are Ala194, Arg145, Arg197, Asp108, Gln459, Glu425, His146, Lys190, Phe149, Pro147 and Tyr148. Docking results of ruthenium complexes are shown in Fig. 3-4 and possible binding interaction of ruthenium complexes with the receptor in terms of hydrogen bond and metal-receptor interaction are presented in Table 4. Fig. 3 shows the binding interaction of **I** and **III** at the surface binding site of subdomain 1B. Complex **I** form a hydrogen bonding interaction with the amino acid residue Gln459 at a distance of about 1.90 Å through its DMSO oxygen atom and a metal receptor interaction is observed with the His146 residue at a distance of about 3.00 Å. A similar orientation is observed for docked structure of complex **III** as it shows a hydrogen bonding interaction with the amino acid residue Gln459 (1.93 Å) and a metal receptor interaction with the residue His146(4.05 Å). Fig. 4 presents the docked structure of complex **II** and complex **IV** at the active site of the protein receptor. Two hydrogen bonding interaction of the complex **II** with amino acid residue His146 (1.69 Å) and Lys190 (2.79 Å) have been observed through its DMSO oxygen atom and imidazolium hydrogen atom while only a single hydrogen bonding interaction is observed for complex **IV** with Glu425 residue at a distance of 2.32 Å. Both the complexes form metal receptor interaction with His146 and Ser193 within a distance of 3.05 Å. As it is observed, the interaction between ruthenium complexes and HSA is not completely hydrophobic in nature since there are several ionic (Asp108, Glu425, Arg145, Arg197 and Lys190) and polar residues (His146, Ser193, Tyr148 and Gln459) in the proximity of the bound ligand (within 4 Å) playing crucial role in stabilizing ruthenium complexes via hydrogen bonding and electrostatic interactions.

ONIOM study

Structural Characteristics

The fully optimized structures of all the adducts of ruthenium complexes with **HSA** calculated at UB3LYP/ 6-31G (d,p): UFF level are shown in Fig. 5 and significant geometrical parameters are listed in Table 5.

Monoaqua interaction:

From Fig. 5 and Table 5, it is seen that inside the binding site of **HSA**, complex **I** has retained its pseudooctahedral configuration, in which water ligand has been replaced from the system by histidyl residue and coordinated with the ruthenium atom at a distance (Ru—N_{His}) of 2.18Å. The Ru—Cl bond lengths are in the range of 2.38-2.42 Å whereas Ru—N and Ru—S bond lengths are 2.11 and 2.43 Å, respectively. It is also observed that complex **I** forms a hydrogen bond between DMSO oxygen atom and one of the hydrogen atoms of glutamine side chain. The existence of the hydrogen bonding in this

RSC Advances Accepted Manuscript

adduct is indicated by the two important aspects: (i) short DMSO—H_{Gln}, contact distance of 2.03 Å (ii) deviations of Cl1—Ru— N_{His} (85.7°) and Cl2—Ru— N_{His} (88.1°) bond angle from the octahedral 90° value. Presences of hydrogen bonding gives additional stability to this adduct. The calculation shows that the dihedral angle Cl3—Cl2—N_{His}—C of **I–HSA** is 91.5^0 which indicate that histidyl ring is found to be perpendicular to the molecular plane about its central axis. Electronic structures of **I–HSA** and **III–HSA** are found to be similar but Ru—N_{His} bond is slightly longer in **III**–HSA, indicating a weaker coordination ability of complex **III** as compared to complex **I**. The dihedral angle Cl3—Cl2—N_{His}—C of **III–HSA** is found to be 47.6^0 reflecting a deviation of histidyl ring from molecular plane.

Diaqua interaction

In **II–HSA,** the ruthenium atom is coordinated with histidyl nitrogen atom and oxygen atom of serine residue of protein receptor at a distance of 2.18 and 1.89 Å. The angle Cl1—Ru—N_{His} is 84.1^0 whereas the angle O_{Ser}—Ru— N_{His} is 88.8^0. This observed deviation of bond angles from 90^0 clearly indicates a distortion of geometry from regular octahedral structure. Complex **II** form two intermolecular hydrogen bonding with the protein receptor: DMSO—H_{His} at 2.06 Å and ImidazoliumCH—O_{Lys} at 2.28 Å. The geometrical parameters of **II–HSA** and **IV–HSA** are almost similar but the latter one is stabilized by presence of two additional hydrogen bonding with glutamic acid residue via imidazolium hydrogen atom. The dihedral angle (Cl3—O—N_{His}—C) of **II–HSA** is found to be 116.7^0 and for **IV-HSA** is 94.7^0.

Stability

In order to find out the stability of the four adducts we have evaluated the binding energy which are presented in Table 6 along with the absolute energy values of the interacting moieties. These results shown in Table 6 allow us to conclude that the binding energies of diaqua adducts are higher than that of monoaqua adducts. That is diaqua adducts are more stable than the corresponding monoaqua adducts. Again, **IV–HSA** have lowest absolute energy value ($\Delta E_{HSA/Ru-complex}$), suggesting that this diaqua form of amino derivative of NAMI-A has higher reactivity towards protein receptor, in agreement with the experimental studies reported by Grossl *et al*.[58] This is mainly due to the presence of primary amine group in this derivative which favors formation of hydrogen bonding interaction towards protein residues, making protein—complex conjugation. In spite of its higher reactivity towards protein receptor, the evaluated binding energy of **IV–HSA** adduct is lower as compared to **II–HSA** and hence exhibited less stability than that of **II–HSA**. **II–HSA** having energy 958.50×10^2 kcalmol^{-1} being the most stable adduct followed by **IV–HSA, I–HSA** and **III–HSA**.

Since all biological interactions are occur in aqueous environments, we have carried out single point calculations on interacting part of all the four adducts to get an estimate of the solvent effect. Inclusion of solvent effect in energy calculations lead to changes in energy and stability of the corresponding adducts. The order of binding energy in aquous solution is found to be in the order: **II–**

RSC Advances Accepted Manuscript

HSA> IV–HSA> **I–HSA**> **III–HSA**. The binding energies of all adducts are evaluated to be higher compared to their respective counterpart in gas phase, indicating the increased stability of all the adducts with the inclusion of solvent medium.

Conclusion

Molecular docking and QM/MM calculation has been carried out for monoaqua and diaqua ruthenium (III) complexes in order to evaluate the binding affinity and stability of the complexes in protein environment. Molecular docking simulation shows that diaqua adduct i.e. **II–HSA** and **IV–HSA** has exhibited higher binding affinity than the corresponding monoaqua adducts (**I–HSA** and **III–HSA**). These studies reveal that in the active site of protein, residues Ala194, Arg145, Arg197, Asp108, Gln459, Glu425, His146, Lys190, Phe149, Pro147 and Tyr148 play a key role in binding with the complexes. In monoaqua adducts, ruthenium complex are found to interact with His146 and Gln459 while ruthenium complexes in diaqua adducts interact with Ser193, Lys190 and Glu425 in addition to His146. Again, two layer ONIOM calculations analyze the stability and energetic details of the interacting ruthenium complexes with protein. The binding energy evaluated by ONIOM calculation suggests the highest stability of **II–HSA** adduct. However, interaction energy of **IV–HSA** adduct is higher than other adduct indicating higher reactivity of complex **IV** towards protein, in agreement with experimental data. Binding energy values suggest that diaqua adducts is more stable than monoaqua adducts. Presence of more hydrogen bonding in diaqua adducts gives extra stability as compared to monoaqua adducts. In addition, the interaction energies of all the four adduct increases in water solvent.

Acknowledgement:

Author Paritosh Mondal thanks Department of Science and Technology (DST), New Delhi, India for financial support (SR/FT/CS-86/2010). Dharitri Das is thankful to the University Grants Commission (UGC), New Delhi for providing research fellowship. Abhijit Dutta is thankful to the DST – SERB project, New Delhi for providing research fellowship.

References

1. V. Bravec and Kasparkova, *Drug Resist. Updat.*, 2005, **8**, 131-146.
2. I. Kostova, *Curr. Med. Chem.*, 2006, **13**, 1085-1107.
3. D.-L. Ma, L.-J. Liu, K.-H. Leung, Y.-T. Chen, H.-J. Zhong, D. S.-H. Chan, H.-M. D. Wang and C.-H. Leung, *Angew. Chem. Int. Ed.,* 2014, **53**, 1 – 6.
4. H.-J. Zhong, K.-H. Leung, L.-J. Liu, L.Lu, D.S.-H. Chan, C.-H. Leung and D.-L. Ma, *ChemPlusChem*, 2014, **79**, 508 – 511.
5. M. A. Jakupec, M. Galanski and B. K. Keppler, *Rev. Physiol. Biochem. Pharmacol.*, 2003**, 146**, 1-54.

RSC Advances Accepted Manuscript

6. Z. Travnicek, M. Matikova-Malarova, R. Novotna, J. Vanco, K. Stepankova and P. Suchy, *J. Inorg. Biochem.*, 2011,**105**, 937-948.

7. T. Pieper, K. Borsky and B. K. Keppler, *Topics Bioinorg. Chem.*, 1999**, 1**, 171-199.

8. G. Sava, E. Alessio, A. Bergamo and G.Mestroni, *Topics Bioinorg. Chem.*, 1999, **1**, 143-169.

9. M. Bouma, B. Nuijen, M. T. Jansen, G. Sava, A. Flaibani, S. Bult and J. H. Beijen, *J. Pharm. Biomed. Anal.*, 2002**, 30**, 1287-129.

10. J .Reedijk, *Curr. Opin. Chem. Biol.*, 1999, **3**, 236-240.

11. M. Bacac, A.C.G. Hotze, K. van der Schilden, J.G. Haasnoot, S. Pacor, E. Alessio, G. Sava and J. Reedijk, *J. Inorg. Biochem*., 2004, **98**, 402–412.

12. M. Brindell, I. Stawoska, J. Supel, A. Skoczowski, G. Stochel and R. van Eldik, *J. Biol. Inorg. Chem*., 2008, **13**, 909–918.

13. M. Bouma, B. Nuijen, M.T. Jansen, G. Sava, A. Flaibani, A. Bult and J.H. Beijnen, Int. J. Pharm., 2002, **248**, 239–246.

14. M. Webb and C. Walsby, *Dalton Trans*., 2011, **40**, 1322–1331.

15. M. Groessl, C.G. Hartinger, P.J. Dyson and B.K. Keppler, *J. Inorg. Biochem.*, 2008, **102**, 1060−1065.

16. V. Brabec and O. Novakova, *Drug Resistance Update*, 2006, **9**, 111-122.

17. O. Novakova, J. Kasparkova, O. Vrana, P. M. Van Vliet, J. Reedijk and V. Brabec, *Biochemistry* 1995, **34**, 12369-12378.

18. C. G. Kuehn and H. Taube, *J. Am. Chem. Soc.*, 1976, **98**, 689. S .Fruhauf and W. Zeller, *Cancer Res.* 1991, **51**, 2943-2948.

19. K. Hindmarsh, D.A. House and M.M. Turnbull, *Inorg. Chim. Acta*., 1997, **257**, 11–18.

20. L.G. Marzilli, S.O. Ano, F.P. Intini and G. Natile, *J. Am. Chem. Soc.*, 1999, **121**, 9133–9142.

21. J. Arpalahti, M. Mikola and S. Mauristo, *Inorg. Chem.*, 1993, **32**, 3327–3332.

22. L. Messori, F.Gonzales Vilchez, R. Vilaplana, F. Piccioli, E. Alessio and B. K. Keppler, *Met.-Based Drugs*., 2000, **7**, 335-342.

23. F. Piccioli, S. Sabatini, L. Messori, P. Orioli, C. G. Hartinger and B. K. Keppler, *J. Inorg. Biochem.*, 2004, **98**, 1135-1142.

24. P. T. Gomme, K. B McCann and K. B Bertolini, J. *Drug Discovery Today,* 2005, **10**, 267-273.

25. E. Reisner, V. B. Arion, C. G. Hartinger, M. A. Jakupec, A. J. L. Pombeiro and B. K. Keppler, n-Wrocław, 2005; Vol. 9, pp 215-229.

26. K. Polec-Pawlak, J. K. Abramski, O. Semenova, C. G. Hartinger, A. R. Timerbaev and B. K Keppler, M Jarosz, *Electrophoresis*, 2006, **27**, 1128-1135.

RSC Advances Accepted Manuscript

27. M. J. Clarke, F. Zu and D. R. Frasca, *Chem. Rev.*, 1999, **99**, 2511-2533.

28. M. J. Clarke, *Coord. Chem. Rev.*, 2002, **232**, 69-93.

29. D. Frasca and M. J. Clarke, *J. Am. Chem. Soc.*, 1999, **121**, 8523-8532.

30. M. Zhao and M. J. Clarke, *J. Biol. Inorg. Chem.*, 1999, **4**, 318-340.

31. C. A. Smith, A. J. Sutherland-Smith, B. K. Keppler, F. Kratz and E. N. Baker, *J. Biol. Inorg. Chem.*, 1996, **1**, 424-431.

32. A. Casini, C. Temperini, C. Gabbiani, C. T. Supuran and L. Messori, *ChemMedChem.*, 2010, **3**, 1989-1994.

33. A. Vergara, G. D'Errico, D. Montesarchio, G. Mangiapia, L. Paduan and A. Merlino, *Inorg. Chem.*, 2013, **52**, 4157-4159.

34. J-C. Chen, L-M. Chen, L-C. Xu, K-C. Zheng and L-N. Ji, *J. Phys. Chem. B*, 2008, **112**, 9966–9974.

35. N. Besker, C. Coletti, A. Marrone and N. Re, *J. Phys. Chem. B*, 2007, **111**, 9955-9964.

36. J. Chen, L. Chen, S. Liao, K. Zheng and L. Ji, *J. Phys. Chem. B*, 2007, **111**, 7862-7869.

37. S. Banerjee and A. K. Mukherjee, *Inorg. Chim. Acta.,* 2013, **400**, 130–141.

38. Q. Fu, L. Zhou and J. Li, *Struct Chem*, 2012, **23**, 1931–1940.

39. P. Sarmah and R.C Deka, *J Mol Struct: Theochem*, 2010, **955**, 53-60.

40. T. Yoshida, Y. Munei, S. Hitaoka, and H. Chuman, *J. Chem. Inf. Model.*, 2010, **50**, 850–860.

41. J. H. A-Morales , J. Caballero , F. D. G-Nilo, R. Contreras, *Chem. Phys. Lett.,*2009, **479**, 149-155.

42. J. H. A-Morales , J. Caballero, A. V. Jague, and F. D. G-Nilo, *J. Chem. Inf. Model.*, 2009, **49**, 886–899.

43. A. D. Becke, *Phys. Rev. A*, 1988, **38**, 3098-3100.

44. C. Lee, W. Yang and R. G. Parr, *Phys. Rev.,* 1988, **37**,785-789.

45. P. J. Hay and W. R. Wadt, *J. Chem. Phys.,* 1985, **82**, 270-284.

46. P. C. Hariharan and J. A. Pople, *Chem. Phys. Lett.,* 1972, **16**, 217-219.

47. M. J. Frisch, G. W. Trucks, H. B. Schlegel, G. E. Scuseria, M. A. Robb, J. R. Cheeseman, G. Scalmani, V. Barone, B. Mennucci, G. A. Petersson, H. Nakatsuji, M. Caricato, X. Li, H. P. Hratchian, A. F. Izmaylov, J. Bloino, G. Zheng, J. L. Sonnenberg, M. Hada, M. Ehara, K. Toyota, R. Fukuda, J. Hasegawa, M. Ishida, T. Nakajima, Y. Honda, O. Kitao, H. Nakai, T. Vreven, J .A. Montgomery, J. E. Peralta, F .Ogliaro, M. Bearpark, J. J. Heyd, E. Brothers, K. N. Kudin, V. N. Staroverov, T. Keith, R. Kobayashi, J. Normand, K. Raghavachari, A. Rendell, J. C. Burant, S. S. Iyengar, J .Tomasi, M. Cossi, N. Rega, J. M. Millam, M. Klene, J.E. Knox, J. B. Cross, V. Bakken, C. Adamo, J. Jaramillo, R. Gomperts, R. E. Stratmann, O. Yazyev, A. J. Austin,

RSC Advances Accepted Manuscript

R.Cammi, C. Pomelli, J. W. Ochterski, R. L. Martin, K. Morokuma, V. G. Zakrzewski, G. A. Voth, P. Salvador, J. J. Dannenberg, S. Dapprich, A. D. Daniels, O. Farkas, J. B. Foresman, J. V. Ortiz, J. Cioslowski and D. J. Fox, Gaussian 09 (Revision B.01), Gaussian Inc., Wallingford, CT, 2010.

48. D.C. Carter and J.X. Ho, *Adv. Protein Chem.*, 1994, **45**, 153–203.

49. G. Sudlow, D.J. Birkett and D.N. Wade, *Mol. Pharmacol.*, 1976, **12**, 1052–1061.

50. K. Tang, Y-M. Qin, A-H. Lin, X. Hu and G.-Lin Zou, *J. Pharm. Biomed. Analysis*, 2005, **39**, 404–410.

51. S. N. Khana, B. Islama, R. Yennamalli, A. Sultana, N. Subbarao and A. U. Khana, *Eur. J. Pharm Sc.*, 2008, **35**, 371–382.

52. G. M. Morris, R. Huey, W. Lindstrom, M. F. Sanner, R. K. Below, D. S. Goodsell and A. Olson J, *J. Comput. Chem.*, 2009, **30**, 2785-2791.

53. V. Barone and M. Cossi, *J. Phys. Chem. A*, 1998, **102**, 1995-2001.

54. M. Cossi, N. Rega, G. Scalmani and V. Barone, *J. Comp. Chem*., 2003, **24**, 669-681.

55. J.I. Aihara, *J. Phys. Chem. A*, 1999, **103**, 7487–7495.

56. R. G. Pearson, Dowden, Hutchinson, Ross, Stroudsburg, PA, 1973.

57. R.G. Pearson, *J. Chem. Educ*., 1987, **64**, 561–567.

58. M. Grossl, E. Reisner, C. G. Hartinger, R. Eichinger, O. Semenova, A. R. Timerbaev, M. A. Jakupec, V. B .Arion and B. K. Keppler, *J. Med. Chem.*, 2007,**50**, 2185-2193.

RSC Advances Accepted Manuscript

Table1. Selected bond lengths (Å) and bond angles (^{0}) calculated for complex **I** and complex **II** at B3LYP level in the gas phase

Parameters	**I**	**II**	**III**	**IV**
Ru—Cl_1	2.43	2.34	2.41	2.32
Ru—Cl_2	2.38		2.41	
Ru—Cl_3	2.34	2.31	2.33	2.30
Ru—Cl_4				
Ru—O(wat1)	2.21	2.23	2.24	2.24
Ru—O(wat2)		2.16		2.18
Ru—N1	2.10	2.10	2.10	2.09
Ru—S_1	2.36	2.41	2.36	2.41
N_1—Ru—S_1	176.3		176.1	175.5
Cl_1—Ru—Cl_2				
Cl_1—Ru—O(wat1)	80.6	83.9	85.1	85.6
O(wat1)—Ru—Cl_2	86.3		80.5	
O(wat1)—Ru—O(wat2)		85.5		82.5
O(wat2)—Ru—Cl3		91.2		90.1
Cl_2—Ru—Cl_3	97.2		97.6	
Cl_3—Ru—Cl_1	95.7	99.8	96.9	99.9

Table2. Energies of HOMO (E_H in eV) and LUMO (E_L in eV) and chemical hardness (η in eV) of ruthenium (III) complexes

Complex	E_H	E_L	ΔE	η
I	-6.204	-3.646	2.558	1.279
II	-10.095	-7.335	2.758	1.379
III	-6.177	-3.646	2.531	1.266
IV	-9.905	-7.510	2.395	1.198

RSC Advances Accepted Manuscript

Table3. Binding energy (ΔE in kcal mol^{-1}) and binding constant (k_b in min^{-1}) of all the complexes with **HSA**, evaluated by molecular docking.

Adducts	ΔE	K_b (experimental data)
I-HSA	-4.52	0.210
II-HSA	-4.74	
III-HSA	-4.58	0.436
IV-HSA	-4.91	

Table 4. Hydrogen bond and metal-receptor interaction of complex **I** and complex **II** with **HSA** evaluated by docking analysis

		Amino acid residue involved in hydrogen bonding
Adducts	Groups	**HSA** amino acid residue
I–HSA	DMSO O atom	HNGln459(1.90Å)
	Metal-receptor	N-imidazole His146(3.00Å)
II–HSA	DMSO O atom	HCH_2His146(1.69Å)
	Imidazolium H atom	O Lys190(2.79 Å)
	Metal-receptor	N-imidazole His146(3.05Å)
	Metal-receptor	OSer193(2.15Å)
III–HSA	DMSO O atom	HNGln459(1.93Å)
	Metal-receptor	N-imidazole His146(4.05Å)
IV–HSA	Metal-receptor	N-imidazole His146(3.03Å)
	Metal-receptor	OSer193(2.57Å)
	Imidazole H atom	O Glu425(2.32 Å)

RSC Advances Accepted Manuscript

Table5. Calculated bond length (Å) and bond angles (^{0}) of monoaquated and diaquated adduct

	I-HSA		III-HSA		II-HSA		IV-HSA	
	Ru-coordination	Hydrogen bonding	Ru-coordination	Hydrogen Bonding	Ru-coordination	Hydrogen bonding	Ru-coordination	Hydrogen bonding
Ru—N_{His}	2.18		2.25		2.18		2.16	
Ru—O_{Ser}					1.89		1.99	
Ru—Cl1	2.42		2.45		2.38		2.38	
Ru—Cl2	2.40		2.38					
Ru—Cl3	2.38		2.36		2.34		2.47	
Ru—S	2.43		2.42		2.48		2.37	
Ru—N	2.11		2.10		2.14		2.16	
DMS<u>O</u>—H_{Gln}		2.03		1.98				
DMS<u>O</u>—H_{His}						2.06		2.43
ImidazoliumC<u>H</u>—O_{Lys}						2.28		
DMSOCH_2<u>H</u>—O_{Ser}						2.50		2.28
ImidazoliumN<u>H</u>—O_{Glu}								1.88
ImidazoliumC<u>H</u>—O_{Glu}								2.04
Cl1—Ru— N_{His}	85.7		87.2		84.1		94.9	
Cl2—Ru— N_{His}	88.1		93.5					
Cl2—Ru— Cl3	92.8		91.5					
Cl3—Ru— Cl1	93.4		87.8		92.6		85.2	
O_{Ser}—Ru— N_{His}					88.8		87.8	
O_{Ser} —Ru— Cl3					95.5		92.1	
Cl3—Cl2—N_{His}—C	91.5		47.6					
Cl3—O—N_{His}—C					116.7		94.7	

RSC Advances Accepted Manuscript

Table 6. Absolute energy values (in au) of interacting adducts and calculated binding energy ($\Delta E \times 10^2$ in $kcalmol^{-1}$) of ruthenium complexes with **HSA** calculated by two layer ONIOM method in gas phase. Interacting part of **HSA** in aqueous phase is calculated by high level UB3LYP/(LANL2DZ+6-31G(d,p)) method.

Adduct	Gas phase				Solvent phase			
	$\Delta E_{HSA/Ru-comple.}$	ΔE_{HSA}	$\Delta E_{Ru-complex}$	ΔE	$\Delta E_{HSA/Ru-complex}$	ΔE_{HSA}	$\Delta E_{Ru-complex}$	ΔE
I–HSA	-3333.57	-1080.52	-2330.49	479.67	-3334.66	-1080.58	-2330.52	479.70
II–HSA	-3087.34	-1293.53	-1946.47	958.50	-3087.34	-1293.65	-1946.56	959.23
III–HSA	-3405.91	-1080.52	-2401.83	479.62	-3405.99	-1080.58	-2401.86	479.69
IV–HSA	-3538.64	-1672.88	-2017.81	954.12	-3538.68	-1672.92	-2017.98	954.68

RSC Advances Accepted Manuscript

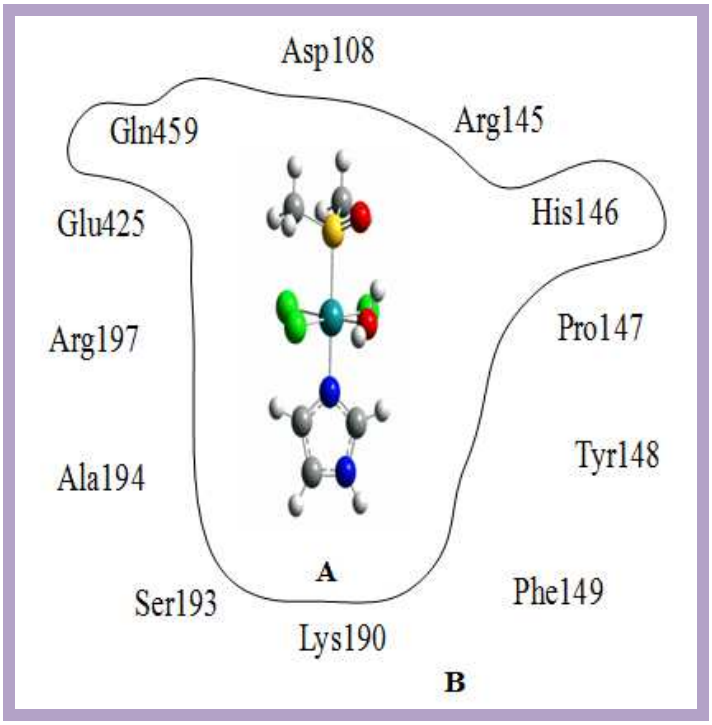

Fig.1. Schematic 2D diagram of the model system for ruthenium complex bound to **HSA** binding site. Layers that are partitioned are shown for ONIOM2 calculations. **A** is the inner layer (QM calculations) and **B** is the outer layer (MM calculations). The arrangement of the residues shown in 2D diagram is not their actual position in 3D.

RSC Advances Accepted Manuscript

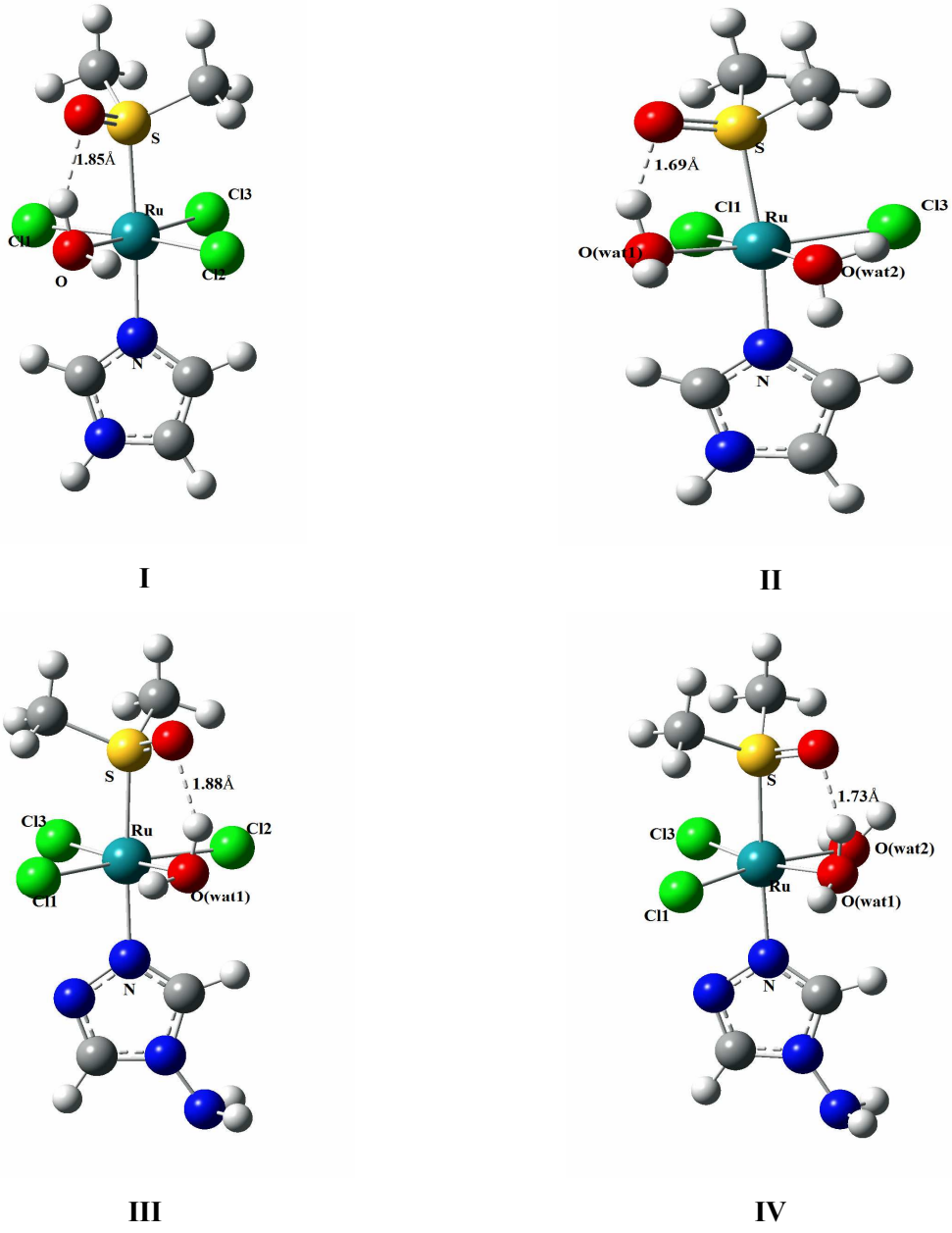

Fig.2. Optimized geometries of complex **I** and complex **II** with appropriate numbering obtained from B3LYP/ (LanL2DZ+6-31G**) calculation.

RSC Advances Accepted Manuscript

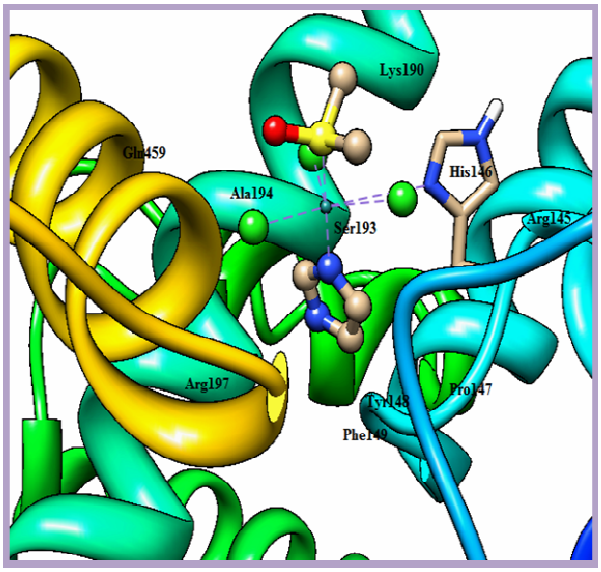

I–HSA

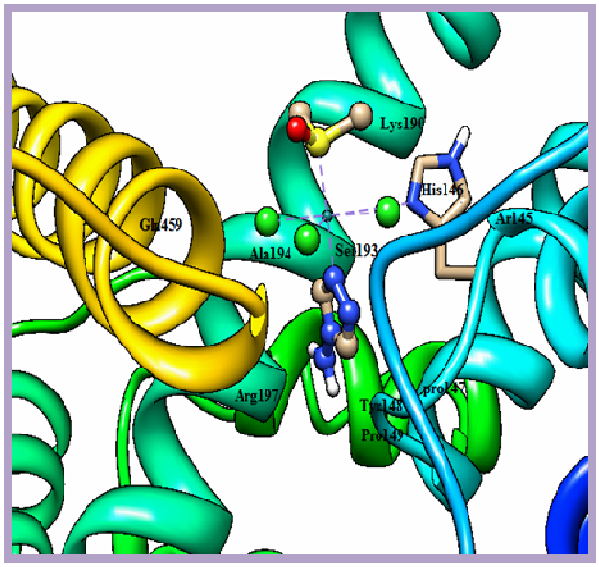

III–HSA

Fig.3. Docked structures of monoaqua complex **I** and complex **II** at the active site of protein receptor. The rest part of protein structure is not shown for clarity.

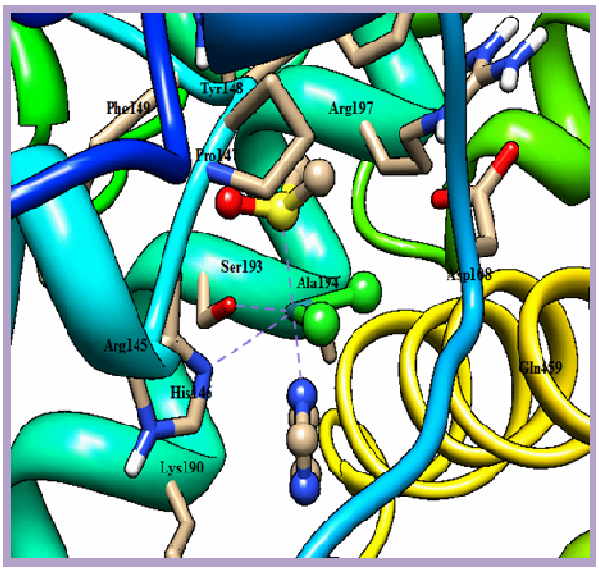

II–HSA

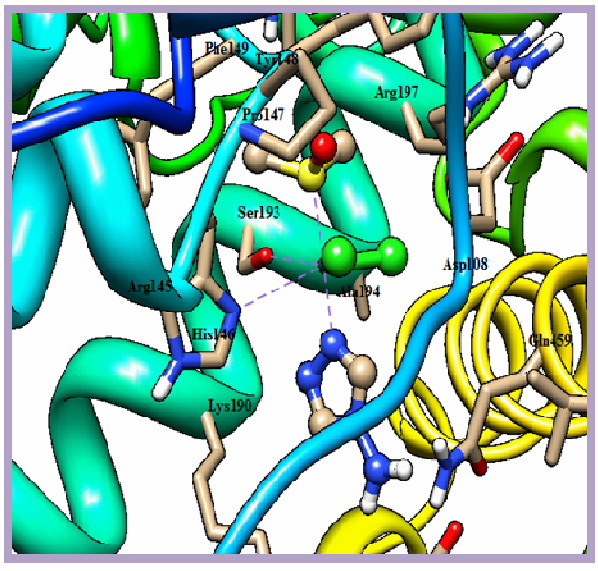

IV–HSA

Fig.4. Docked structures of diaquated adducts at the active site of protein receptor. The rest part of protein structure is not shown for clarity

RSC Advances Accepted Manuscript

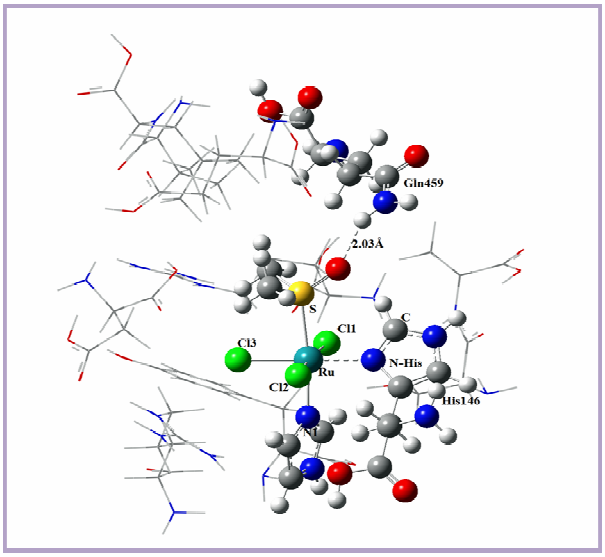

I–HSA

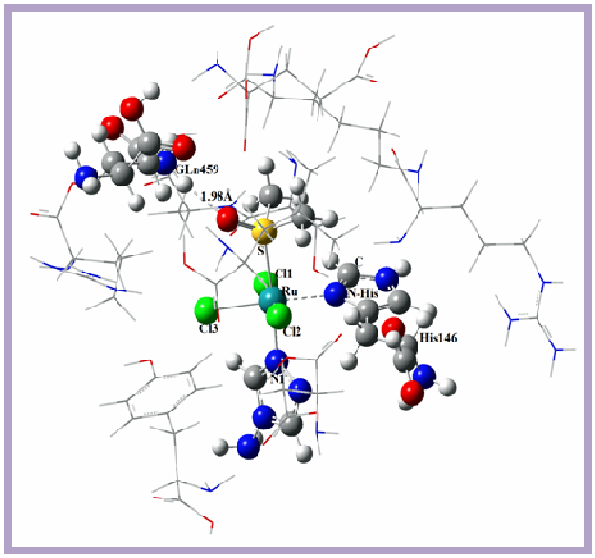

III–HSA

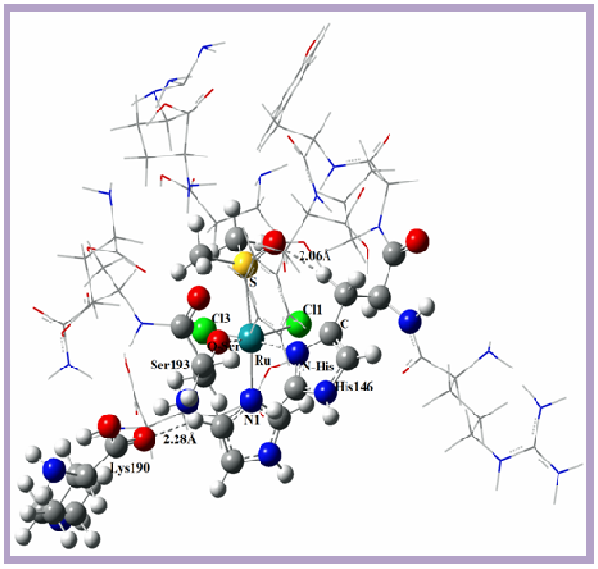

II–HSA

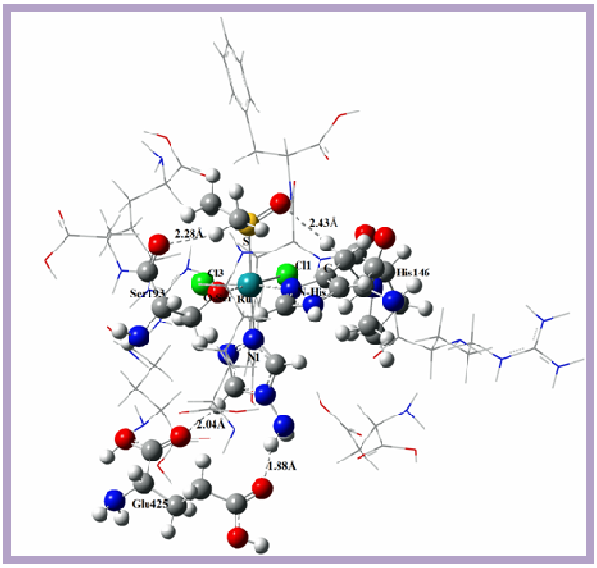

IV-HSA

Fig.5. Optimized geometries of monoaquated and diaquated addcuts with appropriate numbering obtained from two layer QM/MM method.

RSC Advances Accepted Manuscript